JOURNAL OF AGRICULTURAL AND FOOD CHEMISTRY

ARTICLES

Fluorescence-Based Method, Exploiting Lipofuscin, for Real-Time Detection of Central Nervous System Tissues on Bovine Carcasses

HOLGER SCHÖNENBRÜCHER,[†] RAMKRISHNA ADHIKARY,[‡] PRASUN MUKHERJEE,[‡] THOMAS A. CASEY,[§] MARK A. RASMUSSEN,[§,||] FRANK D. MAISTROVICH,[‡] AMIR N. HAMIR,[†] MARCUS E. KEHRLI, JR.,[†] JÜRGEN A. RICHT,*[,†] AND JACOB W. PETRICH*[,‡]

Virus and Prion Diseases of Livestock Research Unit and Pre-Harvest Food Safety and Enteric Disease Research Unit, National Animal Disease Center, Agricultural Research Service, United States Department of Agriculture, Ames, Iowa 50010, and Department of Chemistry, Iowa State University, Ames, Iowa 50011-3111

The removal of central nervous system (CNS) tissues as part of bovine spongiform encephalopathy (BSE) risk material is one of the highest priority tasks to avoid contamination of the human food chain with BSE. No currently available method enables the real-time detection of possible CNS tissue contamination on carcasses during slaughter. The fluorescent pigment lipofuscin is a heterogeneous, high-molecular weight material that has been shown to be enriched in high concentrations in neuronal tissues. In this study, lipofuscin fluorescence was investigated as a marker for real-time detection of CNS contamination. Front-faced fluorescence spectra of brain and spinal cord samples from 11 cattle gave identical, reproducible fluorescence signal patterns with high intensities. The specificity of these spectra was assessed by investigating 13 different non-CNS tissues enabling the differentiation of brain and spinal cord by signal intensity and structure of the spectra, respectively. Small quantities of bovine spinal cord were reliably detected in the presence of raw bovine skeletal muscle, fat, and vertebrae. The presented data are a fundamental basis for the development of a prototype device allowing real-time monitoring of CNS tissue contamination on bovine carcasses and meat cuts.

KEYWORDS: Real-time detection; fluorescence spectroscopy; central nervous system tissues; BSE risk material; lipofuscin; in-process control; food safety

INTRODUCTION

Bovine spongiform encephalopathy (BSE) is a fatal, neurodegenerative transmissible spongiform encephalopathy (TSE) in cattle that is thought to be the cause of variant Creutzfeldt−Jakob disease (vCJD) in humans (*1*). The oral route of infection is considered to be the most likely way of transmission of BSE to humans (*2, 3*). Since most BSE cases were diagnosed in the U.K. and other European countries, the global nature of BSE was highlighted by detection of the disease in cattle in North America (*4, 5*) and Japan (*6*).

Removal of bovine SRMs (e.g., brain and spinal cord) from the human food chain is of critical importance for protecting consumers from BSE (*7, 8*). Brain and spinal cord from BSE infected cattle have been shown to contain the highest infectivity titer of the causative agent of BSE, the abnormal prion protein PrP^{BSE} (*7*). As a consequence, many countries have banned bovine CNS tissues from meat and meat products (constituted by the European commission in Annex V Commission Regulation (EC) No. 999/2001 and for the U.S. in Docket 03-025IF of the USDA FSIS).

Thus far, only laboratory methods for the detection of CNS tissues as part of the BSE risk material have been developed. These include immunochemical detection and ELISA (*9, 10*), gas chromatography−mass spectrometry (GC−MS) (*11*), Western blot analysis (*12, 13*), immunohistochemical methods (*14, 15*), and a real-time reverse transcription (RT)-PCR assay (*16, 17*). None of these methods is suitable for the direct real-time

* To whom correspondence should be addressed. E-mail: (J.A.R.) juergen.richt@ars.usda.gov and (J.W.P.) jwp@iastate.edu.
[†] Virus and Prion Diseases of Livestock Research Unit, USDA.
[‡] Iowa State University.
[§] Pre-Harvest Food Safety and Enteric Disease Research Unit, USDA.
[||] Present address: SarTec Corp., Anoka, MN 55303.

10.1021/jf0734368 CCC: $40.75
Published on Web 07/12/2008

monitoring of CNS contamination on bovine carcasses during slaughter. Real-time-based detection of CNS tissue contamination allows immediate trimming and removal of remaining SRM from the carcass before it enters the food chain. In addition, meat cuts could be monitored after boning to prevent possible contamination with SRM tissues.

Fluorescence spectroscopy commonly is used in a variety of biological applications due to its high sensitivity and specificity (for a review, see refs *18–22*). For example, members of our group previously demonstrated the potential of fluorescence spectroscopy for the detection of fecal contamination on the surface of meat during slaughter (*23, 24*). Here, we discuss the use of the pigment lipofuscin, a heterogeneous, high-molecular weight fluorescent material that has been shown to be enriched in high concentrations in neuronal tissues (*25–30*). Its exact chemical composition is controversial (*25*). In previous steady-state front-faced fluorescence experiments, spectral features consistent with lipofuscin were found in bovine brain and spinal cord (*25, 31*). To investigate the applicability of fluorescence from lipofuscin for a real-time detection of brain and spinal cord, spectral shapes and intensities of these two most important SRM tissues were investigated and compared to 13 non-CNS tissues. Furthermore, the detection sensitivity of bovine spinal cord in the presence of skeletal muscle, fat, and vertebrae was assessed.

MATERIALS AND METHODS

Collection of Bovine Tissue Samples. CNS and non-CNS tissue samples were collected from healthy male ($n = 6$) and female ($n = 5$) cattle directly after slaughter at local abattoirs ($n = 9$) or during necropsy of healthy control animals at the National Animal Disease Center ($n = 2$). All samples remained frozen at −20 °C until processing. Breeds included Holstein ($n = 2$), Simmental ($n = 2$), and Angus cross breeds ($n = 7$). Ages included 2 months ($n = 1$), 5−6 months ($n = 2$), 20−24 months ($n = 4$), and 48−72 months ($n = 4$) as determined by dentition. Brain and spinal cord were investigated as CNS tissues. The 13 non-CNS tissues were adrenal gland, bone (vertebrae), bone marrow, dorsal root ganglia, fat, heart, kidney, liver, lung, lymph node (e.g., iliofemoral ln), peripheral nerve (e.g., sciatic nerve), skeletal muscle, and spleen.

Steady-State Measurements. Steady-state fluorescence spectra were obtained on a SPEX Fluoromax-2 (ISA Jobin-Yvon/SPEX, Edison, NJ) with a 5 nm band-pass and were corrected for lamp spectral intensity and detector response. Fluorescence spectra were collected in a front-faced orientation. To select the appropriate excitation wavelength, brain and spinal cord samples from cattle were excited at 350, 410, 470, and 520 nm. Excitation at 470 nm was determined to provide optimal measurements. Therefore, all samples were excited at 470 nm with an interference filter on the excitation side; emission was collected at wavelengths greater than 505 nm using a cutoff filter before the detector to eliminate scattered light. Polarized fluorescence spectra (not shown) were obtained using two polarizers, one on the excitation side and another on the emission side with an appropriate excitation interference filter and cutoff emission filter. Fluorescence spectra were taken in HH and HV orientations of the polarizers. These spectra were collected to verify that the features observed are not an artifact of scattered light. Statistical and graphical data analysis was performed by using Origin V. Seven software (OriginLab Corp.).

Investigation of Fluorescence Spectra of Bovine Brain, Spinal Cord, and Non-CNS Tissues. Ten identically sized cross and longitudinal sections (five of each) of identical regions of the frontal cortex and the cerebellum of each brain and 10 spinal cord samples from each animal were prepared. Each sample was placed on a microscope slide and stored in a dark moist chamber at ≤7 °C for 120 min until collection of the fluorescence spectra at room temperature. Three cross-sections were prepared for the measurement of the fluorescence signal from each of the cervical, thoracic, lumbar, and sacral regions of the spinal cord from three different animals of 24 months ($n = 2$) and 48 months ($n = 1$) of age. Spinal cord samples from two different animals were kept at −20 °C and used for the collection of fluorescence spectra after 0, 5, 26, 30, 50, and 56 h and 8 weeks. Longitudinal sections and cross-sections of the non-CNS tissues were prepared as described previously.

Sensitivity of Detection of Spinal Cord by Using the Front-Faced Experiment. The lower limit of detection was determined for the optimized setup of the front-faced experiment by using spinal cord cross-sections from two different animals. In general, the total surface area, exposed to excitation light, was 0.4 cm × 1.0 cm. Pieces of each spinal cord cross-section were prepared in duplicate, corresponding to surface areas of 0.4 cm × 0.4 cm and 0.1 cm × 0.2 cm and placed on microscope slides. For each sample, duplicate fluorescence spectra were collected, and the experiment was repeated. The lower limit of detection is defined by convention as the smallest size of tissue that could be detected.

Sensitivity of Detection of Spinal Cord in the Presence of Different Background Tissues. Bovine skeletal muscle, abdominal fat tissues, and vertebrae of two different cattle were used for the assessment of the detection sensitivity of spinal cord in the presence of background tissues. For the front-faced experiments, six sample sections of similar size and height were prepared from these tissues and were placed on microscope slides. Skeletal muscle and fat were cut into pieces of ∼0.2 cm × 0.2 cm. The slices from vertebrae were kept as single pieces that were ∼1.0 cm × 2.0 cm. Cross-sections of spinal cord were prepared from tissues collected from three different animals and prepared as described previously. Separate fluorescence spectra of all background tissue samples and the spinal cord itself were collected initially. Then, a piece of spinal cord was placed among pieces of skeletal muscle or fat and on top of the vertebrae samples, respectively. The sample size of the spinal cord was adjusted to represent fractions of (i) 10% and (ii) 5% of the surface area of the exposed excitation light. The sample size of the spinal cord was adjusted to represent fractions of ∼0.2 cm × 0.2 cm for a surface area of 10% and ∼0.1 cm × 0.2 cm for a surface area of 5%. All artificially spiked samples were prepared in duplicate, and the experiment was conducted twice.

Semiquantitative Measurement of Amount of Spinal Cord Added to Different Background Tissues by Means of Real Time RT-PCR. A comparative analysis using real-time RT-PCR for the detection of ruminant glial fibrillary acidic protein (GFAP) mRNA was performed to (i) show that fat and muscle samples used as background tissues were free of CNS and (ii) show the reproducibility of our spiking experiments by using an alternative CNS detection method described previously (*17*). Threshold cycle values (C_T) obtained for the spiked samples were compared with the C_T values from standards of bovine minced meat artificially spiked with low amounts of bovine spinal cord to quantify the total amount of CNS tissue in each sample. RNA was not isolated from samples with the spinal cord placed on vertebrae.

RESULTS

Selection of Excitation Wavelength. Fluorescence spectra obtained using excitation wavelengths of 350 and 520 nm excitation were weakly fluorescent and noisy, whereas excitation at 410 nm yielded high-intensity spectra containing few characteristic features—namely only one noticeable peak. On the other hand, by using 470 nm as the excitation wavelength, we were able to obtain structured fluorescence spectra with a high signal-to-noise ratio from bovine brain and spinal cord. Therefore, we chose to use 470 nm as the excitation wavelength for all of the samples considered in this study. This is also consistent with observations reported previously (*31*).

Fluorescence Spectra of Bovine CNS and Non-CNS Tissues. The solid CNS and non-CNS tissues fluoresced over a broader range when excited at 470 nm. Characteristic overlaid front-faced fluorescence spectra for CNS (spinal cord and brain) and non-CNS (kidney, dorsal root ganglia, liver, lymph node, peripheral nerve, adrenal gland, lung, fat, heart, vertebrae, skeletal muscle, bone marrow, and spleen) tissues are presented

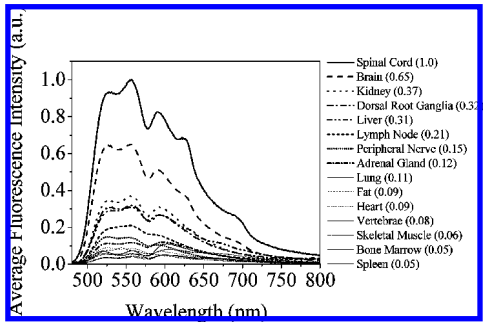

Figure 1. Representative overlaid fluorescence spectra of spinal cord, brain, kidney, dorsal root ganglia, liver, lymph node, peripheral nerve, adrenal gland, lung, fat, heart, vertebrae, skeletal muscle, bone marrow, and spleen. The high fluorescence intensity from the spinal cord enabled the detection of spinal cord in the presence of non-CNS tissue. The values in parentheses represent the average fluorescence intensity with respect to that of the spinal cord, which was arbitrarily taken as unity.

in **Figure 1**. Fluorescence spectra from brain and spinal cord exhibited three prominent peaks centered at ~525, ~555, and 585−600 nm. There were two small shoulders centered at ~625 and ~695 nm. To check as to whether the peaks shown by the spinal cord were not caused by the light scattered from the sample, steady-state fluorescence anisotropy experiments using polarizing filters were undertaken. The HV spectra showed a structure very similar to that of the HH spectra (data not shown). This confirmed that the peaks found in spinal cord were not artifacts of the detection system. Similar results were obtained for brain and non-CNS tissues.

The spectral features of the CNS tissues were highly conserved in all samples studied regardless of age and breed. No differences in the structure and intensity were seen for brain samples taken from cerebrum or cerebellum as well as cervical, thoracic, lumbar, and sacral spinal cord. The possible influence of the storage time and tissue consistency on the fluorescence signal was determined by measuring the fluorescence spectra at different time points and after homogenization, respectively. Reproducible results were obtained even after the storage of spinal cord sections for 0, 5, 26, 30, 50, and 56 h and 8 weeks at −20 °C. A bead beater was used for mechanical homogenization of bovine spinal cord. This did not affect the shape of the spectra but resulted in decreased signal intensity (data not shown). The most apparent difference between the two CNS tissues and all of the non-CNS tissues was the much higher fluorescence intensity obtained for spinal cord and brain tissues (**Figure 1**). This observation strongly suggests that fluorescence techniques can be exploited to differentiate these two tissues from non-CNS samples.

The normalized signal intensity obtained for bovine spinal cord was ~3 times higher than that from kidney and liver and 8−10 times higher than the intensity from skeletal muscle, fat, and vertebrae. Standard errors in fluorescence intensity are shown in **Figure 2**. It is obvious that the spinal cord can easily be detected in the presence of skeletal muscle, fat, and vertebrae since the fluorescence intensity from these background tissues is very low. This might not be true in the presence of kidney, liver, and lymph node tissues.

On the basis of the nature of their fluorescence spectra, the non-CNS tissues offered several other interesting findings. Peripheral nerves and dorsal root ganglia, both part of the peripheral nervous system, as well as the non-CNS tissues liver, kidney, heart, and lymph node showed strong similarities to the spectra of the spinal cord (**Figure 1**). This included the localization of the three peaks with similar relative peak

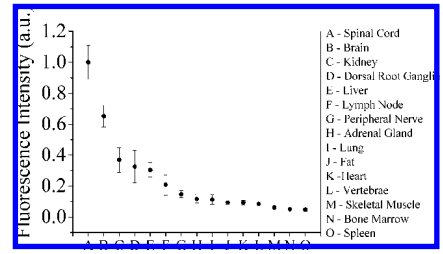

Figure 2. Average fluorescence intensities and corresponding standard errors of CNS and non-CNS tissues from cattle. Intensities were normalized with respect to the maximum average intensity of the spinal cord. All values were calculated with respect to the average fluorescence intensity of the spinal cord, which was arbitrarily taken as unity.

intensities. However, in these non-CNS tissues, the two small shoulders centered at ~625 and ~695 nm were rarely present. Non-CNS tissues such as lung, adrenal gland, fat, skeletal muscle, bone marrow, vertebrae, and spleen showed different fluorescence spectra with regard to relative peak intensity and also peak positions from CNS tissues (**Figure 1**). Lung tissue showed a quite different fluorescence spectrum with peaks centered at ~520 nm, ~555 nm, and a high intense peak at ~600−610 nm relative to the first two peaks. This intense third peak was not observed in CNS and PNS tissues. For adrenal gland and skeletal muscle, the spectra did show three peaks at similar peak maxima like the CNS tissues, but the second and third peak had similar intensities. Fat tissue usually showed spectra with a single peak. A sharp peak at ~545 nm and a sharp shoulder at ~675 nm were detected. Bone marrow showed the three peaks known from CNS tissues, but with a higher intensity for the third peak and an extra broad shoulder at ~655−665 nm. Spleen and vertebrae showed almost similar spectra as compared to that of bone marrow.

Investigation of Detection Sensitivity. The lower limit of detection for bovine spinal cord was addressed for the front-faced fluorescence experiment itself. In addition, the possible interference of the presence of skeletal muscle, fat, and vertebrae on the ability to detect CNS tissue was investigated. The front-faced experiment allowed reproducible collection of spectra described for spinal cord down to a surface area as small as ~0.1 cm × 0.2 cm. Regardless of the presence of skeletal muscle, fat, or vertebrae, 100% detection sensitivity was observed for all of the spinal cord samples representing 10% ($n = 36$) of the entire surface area investigated. By using the experimental setup described previously, 70% of all samples containing a 5% surface area of spinal cord in the background of fat ($n = 12$) and skeletal muscle ($n = 12$) as well as 80% of the samples in the presence of vertebrae ($n = 12$) were identified correctly (**Table 1**). After the addition of 5% spinal cord, the fluorescence intensity was ~1.5 times higher, and characteristic spectra for the spinal cord in the presence of background tissues were observed (**Figures 3** and **4A**−**C**).

All fat and skeletal muscle samples used as background tissues for this experiment were shown to contain no CNS tissues by using real-time PCR analysis. Since solid vertebrae did not permit the possibility of obtaining a homogeneous mixture with spinal cord, the outer surface of these bones was removed to ensure that only a CNS-free background was used. Comparative analysis of fat and skeletal muscle samples containing a 5% surface area of spinal cord by real-time PCR detection of the GFAP mRNA gave concordant results for both consecutive experiments. The C_T values for skeletal muscle spiked with spinal cord were 25.53 (±0.71). Spinal cord in the presence of fat showed C_T values of 21.46 (±1.09) (**Table 1**).

Table 1. Detection Sensitivity (% Surface Area) of Bovine Spinal Cord in the Presence of Different Background Tissues Investigated in Two Separate Experiments for Each Background Tissue[a]

	detection sensitivity (% [*n*]) in presence of background tissues			C_T (±SD)	
surface area (%) of spinal cord	skeletal muscle	fat	vertebrae	skeletal muscle	fat
10	100% (*n* = 12)	100% (*n* = 12)	100% (*n* = 12)	n.d.[b]	n.d.
5	70% (*n* = 12)	70% (*n* = 12)	80% (*n* = 12)	25.53 (±0.71)	21.46 (±1.09)

[a] The 5% surface area of bovine spinal cord tissue in muscle and fat corresponds to a total amount of 5% (skeletal muscle) to 7% (fat) of spinal cord in the prepared samples as determined by real-time RT-PCR amplification of the GFAP mRNA. Threshold cycle C_T values are given for each of the two experiments conducted per tissue. Spinal cord in the background of solid vertebrae slices was not analyzed by real-time PCR because the solid bone did not result in a homogeneous mixture, and the signal obtained from the spinal cord would be overestimated. [b] n.d.: not determined.

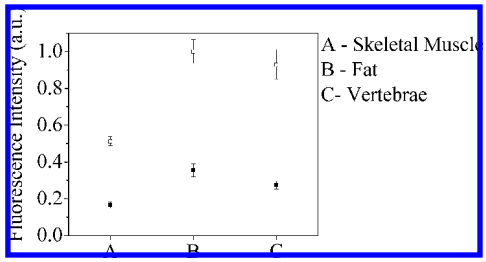

Figure 3. Fluorescence intensities obtained for background tissue skeletal muscle, fat, and vertebrae (solid squares) and in the presence of 5% spinal cord (open squares). The error bars represent the standard errors associated with the measurements. Note that 5% spinal cord can be detected in the presence of skeletal muscle, fat, and vertebrae as background tissue.

DISCUSSION

BSE is a zoonotic disease causally associated with vCJD in humans. BSE epidemic in various parts of the world had a severe impact on livestock and meat trade. Even 20 years after the first identification of the disease, the U.K. estimated costs in 2005−2006 for its BSE control measures including cohort culls and offspring cull compensation of approximately £265 million. Additional administrative costs for inspection and enforcement were estimated to be £64 million as reported for 1999−2000 (*32*). In the U.S., beef exports decreased by over 80% in 2004 after the confirmation of only one BSE case and persisted below pre-2004 levels (*33*). Total U.S. beef industry losses arising from decreased beef and offal exports during 2004 ranged from $3.2 billion to $4.7 billion (*34*). Resumption of beef exports depended on several restrictions made by important trade partners Japan and South Korea. This included the removal of SRM (e.g., brain and spinal cord) and, in the case of South Korea, the acceptance of only boneless products, which represented an important export product for the South Korean market (*33*).

Consumer protection from the spread of BSE to the food chain is based on (i) testing of cattle of particular minimal age for the presence of a BSE infection, (ii) ban of SRM (in particular, brain and spinal cord) from the food chain, and (iii) the ruminant feed ban. The materials identified as bovine SRM are the brain, skull, eyes, trigeminal ganglia, spinal cord, vertebral column (excluding the vertebrae of the tail, the transverse processes, and the wings of the sacrum), DRG from

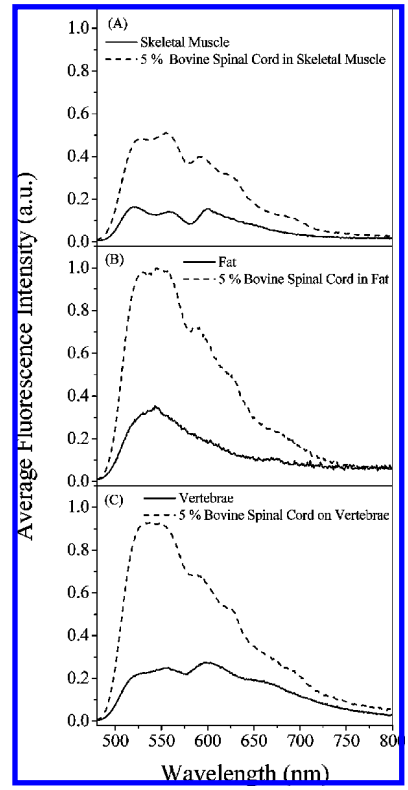

Figure 4. Assessment of the detection sensitivity of 5% surface area of bovine spinal cord in the presence of (**A**) skeletal muscle, (**B**) fat, and (**C**) vertebrae. Excitation and emission conditions are as stated previously. A surface area of 5% spinal cord can be detected in the presence of skeletal muscle, fat, and vertebrae based upon fluorescence spectral shape and intensity. Detection sensitivity is given in **Table 1**.

cattle of 30 months of age and older, and the distal ileum of the small intestine and the tonsils from all cattle (*35*). The 30 month and older age classification for SRMs is accepted by the U.S. and several other countries based on O.I.E. (World Organization for Animal Health) requirements.

Current methods for detecting CNS tissues in meat and meat products are mainly based on ELISA and PCR techniques. The major drawbacks of ELISA (*9, 10*) or real-time PCR (*16, 17*) methods are their high costs and the need for varying degrees of access to laboratory environments and equipment, making them unsuitable for on-site monitoring during the slaughter process. On the other hand, light-based spectroscopic techniques are rapid and noninvasive, requiring no sample preparation. For example, we previously developed a method and apparatus for the real-time detection of fecal contamination on bovine carcasses using fluorescence-based detection of bovine feces containing undesirable bacteria, which has been proven to be a reliable technique (*23, 24*); it is now being adopted in packing plants in the U.S. and France. Using the same principles, we propose to use fluorescent lipofuscin as a marker of CNS tissue (*36*).

Lipofuscin is a high-molecular weight granular yellow−brown substance that is believed to result from oxidative stress of many biomolecules, particularly polyunsaturated fatty acids. It is heterogeneous, highly fluorescent, and undergoes age related progressive accumulation in animal cells, mainly in postmitotic cells, such as neurons, cardiac muscles, and retinal epithelium. Lipofuscin is implicated in many aspects of normal health, including aging, oxidative stress, macular degeneration, lipid peroxidation, as well as some disease processes including

atherosclerosis, dementia (Alzheimer's disease), and prion diseases (*25–30, 37–40*).

We observed in this study that spectra obtained from all solid bovine CNS and non-CNS tissue samples were not contaminated by the artifacts of scattered light. This was consistent with previous findings showing the occurrence of lipofuscin in high concentrations in brain and spinal cord (*31*). Our investigation included male and female cattle at the age of 2−72 months. Since 24 month old bovines represent the largest contingent of slaughtered beef cattle in the U.S. (*41*), special care was taken to include samples of animals of this age in every part of the validation studies. We conclude that the detectability of the fluorescence signal is not affected by nonhomogeneous distribution of lipofuscin that might be age or sex dependent or be observed in different anatomical regions. This is consistent with the chemical stability of lipofuscin (*25*). To give a more detailed analysis of possible age related variations in signal intensity, experiments are underway investigating a large number of age, sex, and breed matched samples. We also found that characteristic CNS tissue fluorescence spectra and intensities could be reliably detected after storage at −20 °C for at least 8 weeks (data not shown). This observation is of special importance for the analysis of possible CNS contamination on meat cuts processed from frozen beef.

The shape of the spectra collected from spinal cord and brain were not tissue specific but also could be found in PNS tissues, liver, kidney, heart, and lymph nodes. In contrast, lung, adrenal gland, skeletal muscle, bone marrow, spleen, and vertebrae could be clearly distinguished with respect to relative peak intensity and in some cases also peak positions. However, the average fluorescence signal intensity of PNS and non-CNS tissues (except kidney and liver) is at least 4−5 times less than that in CNS tissues, offering the potential for the detection of low amounts of spinal cord and brain tissues on bovine carcasses based on different intensities. The presence of spinal cord on skeletal muscle, fat, and vertebrae also can be determined by the different spectral features.

We focused on the detection sensitivity of the spinal cord and the possible influence of different background tissues. Characteristic spectra of spinal cord were reliably detected down to a sample size of ∼0.1 cm × 0.2 cm. It is noteworthy that this low detection sensitivity also enables the detection of small dorsal root ganglia and peripheral nerve cords. Dorsal root ganglia have been classified as SRM, and peripheral nerves have been shown to contain low amounts of PrP^{BSE} in BSE affected cattle (*42, 43*). During slaughter, spinal cord fragments are easily spread over skeletal muscle, fat, and vertebrae, making those tissues the most important non-CNS tissues that were included in the present study. The fluorescent signal collected from 5% surface area of spinal cord and detected in 70% (skeletal muscle and fat) or 80% (vertebrae) of the samples, respectively, was not caused by the entire amount of fluorescent substances present in the sample but only the amount in the two-dimensional (2-D) area exposed to excitation light. This method does not allow comparison with CNS percentage values, which are usually used for semiquantitative measurements by ELISA or real-time PCR methods. The latter test systems refer to the amount of target material contained in the total initial weight and use the 3-D analysis of the entire sample. Therefore, real-time PCR-based detection of GFAP mRNA (*16, 17*) was selected to investigate the quality of the artificially contaminated samples. This method previously showed its accuracy and robustness in a multicenter trial (*44*). Its high tissue specificity and potential for accurate quantification of CNS tissues were proven recently in direct comparison with two commercially available ELISAs (*45*). Since all skeletal muscle and fat tissues were free of CNS tissues as confirmed by PCR analysis, it was proven that the spectra obtained from these tissues were not due to CNS contamination. As indicated by C_T values, all artificially spiked samples were homogeneous preparations containing an entire amount of spinal cord ranging from 5% in muscle to 7% in fat. In comparison, semiquantitative measurements of spinal cord contamination on bovine carcasses varied from 0.5% (*46*) to more than 1% (data not shown). Since the front-faced experiment collects the fluorescence of the CNS tissue located only on a sample surface, the detection sensitivity obtained by fluorescence spectroscopy is actually lower than the detection sensitivity reported by real-time PCR analysis.

The fluorescence spectra of fat and vertebrae not only differed in signal intensity but also in shape. As a consequence, the potential to lower the detection sensitivity can be easily achieved. Similarly, the sensitivity for detection of spinal cord in the presence of skeletal muscle can possibly be increased by comparing the fluorescence signal intensity ratio between the second and the third peak. The third peak always gave a lower signal intensity in the spinal cord but a higher intensity in skeletal muscle.

The present study revealed the potential of fluorescent marker substances, such as lipofuscin, for the real-time detection of spinal cord on bovine carcasses and processed meat cuts including bone-in or boneless products. The front-faced experiments were conducted with a well-standardized, but technologically simple, setup that allowed the detection of small amounts of bovine spinal cord in the presence of fat, skeletal muscle, and vertebrae. Our future work will focus on the development of industrial prototypes such as a hand-held device or entire carcass imaging. Future focus will be on complex mixtures of CNS tissues with background tissues obtained from skeletal muscle, fat, and sawdust of vertebrae and other bones. Real-time monitoring for possible CNS contamination during slaughter would provide an additional, science-based tool for sanitation procedures for the removal of SRM at the abattoir. A benefit to the beef production industry would be an improved product quality assurance and would result in increased consumer protection.

ABBREVIATIONS USED

A.U., arbitrary units; CNS, central nervous system; DRG, dorsal root ganglia; ELISA, enzyme-linked immunosorbent assay; FSIS, Food Safety and Inspection Service; HACCP, hazard analysis and critical control point; HH, horizontal−horizontal; HV, horizontal−vertical; PNS, peripheral nervous system; PCR, polymerase chain reaction; SRM, specified risk material.

ACKNOWLEDGMENT

The support of local slaughterhouses and the Iowa State University Meat Laboratory in sample collection is gratefully acknowledged. We thank Hannah Polashek for technical assistance with RT-PCR analysis.

LITERATURE CITED

(1) Ironside, J. W. Review: Creutzfeldt−Jakob disease. *Brain Pathol.* **1996**, *6*, 379–388.

(2) Cousens, S.; Smith, P. G.; Ward, H.; Everington, D.; Knight, R. S.; Zeidler, M.; Stewart, G.; Smith-Bathgate, E. A.; Macleod, M. A.; Mackenzie, J.; Will, R. G. Geographical distribution of variant Creutzfeldt−Jakob disease in Great Britain, 1994−2000. *Lancet* **2001**, *357*, 1002–1007.

(3) Comer, P. J.; Huntly, P. J. TSE risk assessments: A decision support tool. *Stat. Methods Med. Res.* **2003**, *12*, 279–291.
(4) (a) Richt, J. A.; Kunkle, R. A.; Alt, D.; Nicholson, E. M.; Hamir, A. N.; Czub, S.; Kluge, J.; Davis, A. J.; Hall, S. M. Identification and characterization of two bovine spongiform encephalopathy cases diagnosed in the United States. *J. Vet. Diagn. Invest.* **2007**, *19*, 142–154. (b) Erratum in J. Vet. Diagn. Invest. **2007**, *19*, 454.
(5) Stack, M. J.; Balachandran, A.; Chaplin, M.; Davis, L.; Czub, S.; Miller, B. The first Canadian indigenous case of bovine spongiform encephalopathy (BSE) has molecular characteristics for prion protein that are similar to those of BSE in the United Kingdom but differ from those of chronic wasting disease in captive elk and deer. *Can. Vet. J.* **2004**, *45*, 825–830.
(6) Giles, J. Mad cow disease comes to Japan. *Nature (London, U.K.)* **2001**, *413*, 240.
(7) European Food Safety Authority (EFSA). Quantitative assessment of the residual BSE risk in bovine-derived products, EFSA QRA report 2004: Working document. EFSA J. 2005, *307*, 1−135.
(8) Harvard Risk Assessment of Bovine Spongiform Encephalopathy Update, Phase IA, Harvard Center for Risk Analysis. Harvard School of Public Health. October 31, 2005. Harvard, MA. http://www.fsis.usda.gov/Science/Risk_Assessments/.
(9) Schmidt, G. R.; Hossner, K. L.; Yemm, R. S.; Gould, D. H.; O'Callaghan, J. P. An enzyme-linked immunosorbent assay for glial fibrillary acidic protein as an indicator of the presence of brain or spinal cord in meat. *J. Food. Prot.* **1999**, *62*, 394−397.
(10) Schmidt, G. R.; Yemm, R. S.; Childs, K. D.; O'Callaghan, J. P.; Hossner, K. L. The detection of central nervous system tissue on beef carcasses and in comminuted beef. *J. Food Prot.* **2001**, *64*, 2047–2052.
(11) Biedermann, W.; Lücker, E.; Porschmann, J.; Lachhab, S.; Truyen, U.; Hensel, A. Structural characterization of some fatty acids from the brain as biomarkers of BSE risk material. *Anal. Bioanal. Chem.* **2004**, *379*, 1031–1038.
(12) Villmann, C.; Sandmeier, B.; Seeber, S.; Hannappel, E.; Pischetsrieder, M.; Becker, C. M. Myelin proteolipid protein (PLP) as a marker antigen of central nervous system contaminations for routine food control. *J. Agric. Food Chem.* **2007**, *55*, 7114–7123.
(13) Lücker, E. H.; Eigenbrodt, E.; Wenisch, S.; Failing, K.; Leiser, R.; Bülte, M. Development of an integrated procedure for the detection of central nervous tissue in meat products using cholesterol and neuron-specific enolase as markers. *J. Food. Prot.* **1999**, *62*, 268–276.
(14) Wenisch, S.; Lücker, E.; Eigenbrodt, E.; Leiser, R.; Bülte, M. Detection of central nervous tissue in meat products−An immunhistological approach. *Nutr. Res. (N.Y.)* **1999**, *19*, 1165–1172.
(15) Lücker, E. H.; Eigenbrodt, E.; Wenisch, S.; Leiser, R.; Bülte, M. Identification of central nervous system tissue in retail meat products. *J. Food Prot.* **2000**, *63*, 258–263.
(16) Schönenbrücher, H.; Abdulmawjood, A.; Bülte, M. Neuartiger tierartspezifischer nachweis von GFAP in prozessierten lebensmitteln mit einem real time-PCR-verfahren. *Fleischwirtschaft* **2004**, *6*, 114–117.
(17) Abdulmawjood, A.; Schönenbrücher, H.; Bülte, M. Novel molecular method for detection of bovine-specific central nervous system tissues as bovine spongiform encephalopathy risk material in meat and meat products. *J. Mol. Diagn.* **2005**, *7*, 368–374.
(18) Christensen, J.; Norgaard, L.; Bro, R.; Balling Engelsen, S. Multivariate autofluorescence of intact food systems. *Chem. Rev.* **2006**, *106*, 1979–1994.
(19) Wold, J. P.; Mielnik, M. Nondestructive assessment of lipid oxidation in minced poultry meat by autofluorescence spectroscopy. *J. Food Sci.* **2000**, *65*, 87–95.
(20) Olsen, E.; Vogt, G.; Ekeberg, D.; Sandbakk, M.; Pettersen, J.; Nilsson, A. Analysis of the early stages of lipid oxidation in freeze-stored pork back fat and mechanically recovered poultry meat. *J. Agric. Food Chem.* **2005**, *53*, 338–348.
(21) Olsen, E.; Vogt, G.; Veberg, A.; Ekeberg, D.; Nilsson, A. Analysis of early lipid oxidation in smoked, comminuted pork of poultry sausages with spices. *J. Agric. Food Chem.* **2005**, *53*, 7448–7457.
(22) Wold, J. P.; Mielnik, M.; Pettersen, M. K.; Aaby, K.; Baardseth, P. Rapid assessment of rancidity in complex meat products by front face fluorescence spectroscopy. *J. Food Sci.* **2002**, *67*, 2397–2404.
(23) Ashby, K. D.; Casey, T. A.; Rasmussen, M. A.; Petrich, J. W. Steady-state and time-resolved spectroscopy of F420 extracted from methanogen cells and its utility as a marker for fecal contamination. *J. Agric. Food Chem.* **2001**, *49*, 1123–1127.
(24) Ashby, K. D.; Wen, J.; Chowdhury, P.; Casey, T. A.; Rasmussen, M. A.; Petrich, J. W. Fluorescence of dietary porphyrins as a basis for real-time detection of fecal contamination on meat. *J. Agric. Food Chem.* **2003**, *51*, 3502–3507.
(25) Yin, D. Biochemical basis of lipofuscin, ceroid, and age pigment-like fluorophores. *Free Radical Biol. Med.* **1996**, *21*, 871–888.
(26) Boellaard, J. W.; Schlote, W.; Tateishi, J. Neuronal autophagy in experimental Creutzfeldt−Jakob's Disease. *Acta Neuropathol.* **1989**, *78*, 410–418.
(27) Terman, A.; Brunk, U. T. Lipofuscin: Mechanisms of formation and increase with age. *Acta Pathol., Microbiol., Immunol.* **1998**, *106*, 265–276.
(28) Tsuchida, M.; Miura, T.; Aibara, T. Lipofuscin and lipofuscin-like substances. *Chem. Phys. Lipids* **1987**, *44*, 297–325.
(29) Curtis, H. J. *Biological Mechanisms of Aging*; Charles C. Thomas: Springfield, IL, 1996.
(30) Strehler, B. L. *Time, Cells, and Aging*; Academic Press: San Diego, 1977.
(31) Chowdhury, P. K.; Halder, M.; Choudhury, P. K.; Kraus, G. A.; Desai, M. J.; Armstrong, D. W.; Casey, T. A.; Rasmussen, M. A.; Petrich, J. W. Generation of fluorescent adducts of malondialdehyde and amino acids: Toward an understanding of lipofuscin. *Photochem. Photobiol.* **2004**, *79*, 21–25.
(32) Department for Environment, Food, and Rural Affairs. Animal Health and Welfare: BSE General Question and Answer; 2007; http://www.defra.gov.uk/animalh/bse/index.html.
(33) Vandever, M. Livestock and Meat Trade: A look at the effects of BSE. *Amber Waves* **2007**, *5*, 28–29.
(34) Coffey, B.; Mintert, J.; Fox, J. A.; Schroeder, T.; Valentin, L. *The Economic Impact of BSE on the U.S. Beef Industry: Product Value Losses, Regulatory Costs, and Consumer Reactions*; Kansas State University Agricultural Experiment Station and Cooperative Extension Service: Manhattan, KS, 2005; http://fss.k-state.edu/index.php?option=com_content&task=view&id=28&Itemid=37.
(35) Food Safety and Inspection Service. Prohibition of the use of specified risk materials for human food and requirements for the disposition of non-ambulatory disabled cattle; Prohibition of the use of certain stunning devices used to immobilize cattle during slaughter (9 CFR Parts 309, 310, and 318 [Docket No. 03-025F]). Fed. Regist. 2007, 38700−38730.
(36) Casey, T. A.; Rasmussen, M. A.; Gapsch, A. H.; Flick, R. L.; Petrich, J. W. Real-time monitoring of age pigments and factors relating to transmissible spongiform encephalopathies and apparatus. U.S. Patent Application 10/638.695, 2004.
(37) Sohal, R. S. *Age Pigments*; Elsevier: Amsterdam, 1981.
(38) Terman, A. Garbage catastrophe theory of aging: Imperfect removal of oxidative damage. *Redox Rep.* **2001**, *6*, 15–26.
(39) Mata, N. L.; Weng, J.; Travis, G. H. Biosynthesis of a major lipofuscin fluorophore in mice and humans with ABCR-mediated retinal and macular degeneration. *Proc. Natl. Acad. Sci.* **2000**, *97*, 7154–7159.
(40) Boulton, M.; Docchio, F.; Dayhaw-Barker, P.; Ramponi, R.; Cubeddu, R. Age-related changes in the morphology, absorption, and fluorescence of melanosomes and lipofuscin granules of the retinal pigment epithelium. *Vision Res.* **1990**, *30*, 1291–1303.
(41) Lawrence, T. E.; Whatley, J. D.; Montgomery, T. H.; Perino, L. J. A comparison of the USDA ossification-based maturity system to a system based on dentition. *J. Anim. Sci.* **2001**, *79*, 1683–1690.
(42) Iwata, N.; Sato, Y.; Higuchi, Y.; Nohtomi, K.; Nagata, N.; Hasegawa, H.; Tobiume, M.; Nakamura, Y.; Hagiwara, K.; Furuoka, H.; Horiuchi, M.; Yamakawa, Y.; Sata, T. Distribution of PrP(Sc) in cattle with bovine spongiform encephalopathy

slaughtered at abattoirs in Japan. *Jpn. J. Infect. Dis.* **2006**, *59*, 100–107.

(43) Masujin, K.; Matthews, D.; Wells, G. A.; Mohri, S.; Yokoyama, T. Prions in the peripheral nerves of bovine spongiform encephalopathy-affected cattle. *J. Gen. Virol.* **2007**, *88*, 1850–1858.

(44) Abdulmawjood, A.; Schönenbrücher, H.; Bülte, M. Collaborative trial for validation of a real-time reverse transcriptase-polymerase chain reaction assay for detection of central nervous system tissues as bovine spongiform encephalopathy risk material: Part 1. *J. AOAC Int.* **2006**, *89*, 1335–1340.

(45) Schönenbrücher, H.; Abdulmawjood, A.; Göbel, K. A.; Bülte, M. Detection of central nervous system tissues in meat products: Validation and standardization of a real-time PCR-based detection system. *Vet. Microbiol.* **2007**, *123*, 336–345.

(46) Lücker, E.; Schlottermüller, B.; Martin, A. Studies on contamination of beef with tissues of the central nervous system (CNS) as pertaining to slaughtering technology and human BSE-exposure risk. *Berl. Munch Tierarztl. Wochenschr.* **2002**, *115*, 118–121.

Received for review November 26, 2007. Revised manuscript received May 6, 2008. Accepted May 13, 2008. Mention of trade names or commercial products in this paper is solely for the purpose of providing specific information and does not imply recommendation or endorsement by the U.S. Department of Agriculture.

JF0734368